Revista Mexicana de Astronomía y Astrofísica, **49**, 285–299 (2013)

OPEN CLUSTERS IN CARINA: NGC 3603, WESTERLUND 2 AND SHER 1[1]

Ana María Orsatti,[2,3,4] E. Irene Vega,[2,4] and Ruben E. Martínez[2,3]

Received 2013 May 10; accepted 2013 July 26

RESUMEN

Se presentan observaciones polarimétricas en las bandas $UBVRI$ de estrellas situadas en la dirección de los cúmulos NGC 3603, Westerlund 2 y Sher 1, con el propósito de estudiar las características del polvo entre el Sol y los cúmulos, evidencias polarimétricas de la existencia (o no) de enrojecimiento anómalo en NGC 3603 y en Westerlund 2, y la identificación de estrellas con indicios de polarización intrínseca.

40% de las estrellas observadas en Westerlund 2 presentan indicios de polarización intrínseca, porcentaje similar al encontrado en NGC 6611 y en IC 2944; en cambio, en NGC 3603 es mucho menor. Las eficiencias polarimétricas medias son bajas por la presencia de varias nubes de polvo interestelar entre los objetos y el Sol. Se apoya la existencia de enrojecimiento anómalo en NGC 3603, mientras que en Westerlund 2 existen leves indicios de ello.

ABSTRACT

We present polarimetric observations in the $UBVRI$ bands of stars located in the directions of NGC 3603, Westerlund 2 and Sher 1. Our main objectives are to study the characteristics of the dust lying between the Sun and the clusters, to analyze polarimetric evidence on the existence (or not) of abnormal reddening in NGC 3603 and Westerlund 2; and to identify stars with signatures of intrinsic polarization.

40% of the stars observed in Westerlund 2 display indications of intrinsic polarization, a percentage similar to those found in the open clusters NGC 6611 and IC 2944: but in NGC 3603 it is very small. Mean polarization efficiencies are low, due to the presence of several dust clouds located in the way to the clusters. We are in favor of the existence of abnormal reddening in NGC 3603, while in Westerlund 2 there are only indications.

Key Words: ISM: dust, extinction — open clusters and associations: individual (NGC 3603, Westerlund 2, Sher 1)

1. INTRODUCTION

The polarimetric technique is a very useful tool for obtaining significant information (magnetic field direction, $\lambda_{\max}$, $P_{\lambda_{\max}}$, etc.) about dust located in front of a luminous object. Open clusters are very good candidates for polarimetric observations, because many of them have been studied through photometric and spectroscopic techniques and detailed information on the color, luminosity, spectral type and other properties of their stars is readily available. Thus, the physical parameters of the cluster and its stars can be obtained, and adding polarimetric observations we can study the distribution, size and efficiency of the dust grains which polarize the starlight.

As some of the open clusters spread over a significant area, it is possible to analyze the evolution of

[1]Based on observations obtained at Complejo Astronómico El Leoncito, operated under agreement between the Consejo Nacional de Investigaciones Científicas y Técnicas de la República Argentina and the Universities of La Plata, Córdoba, and San Juan, Argentina.

[2]Facultad de Ciencias Astronómicas y Geofísicas, Observatorio Astronómico, La Plata, Argentina.

[3]Instituto de Astrofísica de La Plata, CONICET, Argentina.

[4]Member of the Carrera del Investigador Científico, CONICET, Argentina.

the physical parameters of the dust over the region. Besides, it is also possible to detect the presence (if any) of intracluster dust and, with additional observations of non-member stars in the same region, to investigate the interstellar dust distribution along the line of sight to the cluster and the different directions of the Galactic magnetic field along that line of sight.

As part of systematic polarimetric observations in a large number of galactic open clusters, undertaken by our working group at La Plata Observatory that includes the study of about 17 objects in the years 1994 to 2013, on this occasion we have selected three of the many open clusters along the Carina arm, located at different distances from the Sun: NGC 3603, Westerlund 2 and Sher 1.

They are young and have in common another characteristic: a very crowded core which prevents observers from performing good photometric and polarimetric observations. Two of them are related to HII regions (NGC 3603, Westerlund 2) and subject of studies to clarify if the normal extinction law, characterized by a value $R_V = 3.1$, is valid there.

NGC 3603 ($l = 291\overset{\circ}{.}62$, $b = -0\overset{\circ}{.}52$) is a very massive optically visible giant HII region with a starburst cluster which ionizes the gas (Goss & Radhakrishnan 1969). The core is composed of very early O-type and H-rich WN + abs stars (Melena et al. 2008). The reddening mean value is large: $E_{B-V} = 1.40$ mag (Moffat 1983); and there is little variation in reddening across the cluster core. Melnick, Tapia, & Terlevich (1989) found a tendency for the reddening to increase slightly with the distance from the center of the cluster, which could be due to the evaporation of dust particles caused by the intense stellar ultraviolet radiation in the central region. The distance of NGC 3603 is a controversial matter: many investigations agree in the value of the distance modulus, but not on the distance. This is due to the unsolved question about the possible existence of anomalous reddening, introduced by Pandey, Ogura, & Sekiguchi (2000), an issue that must be clearly answered.

Westerlund 2 ($l = 284\overset{\circ}{.}27$, $b = -0\overset{\circ}{.}33$) is located toward the outer edge of the Carina arm and embedded in nebulosity. It is believed to be responsible for the core excitation of the HII region RCW 49 (Belloni & Mereghetti 1994). It contains an X-ray source that is either a supernova remnant or a wind-powered X-ray bubble (Goldwurn, Caraveo, & Bignami 1987) and it has a Wolf-Rayet as one of its members, which indicates that the cluster is very young. None of the stars are clearly evolving from the ZAMS and the cluster has a calculated age of less than 2 Myr. Westerlund 2 is a very compact open cluster, and this situation causes severe problems when performing photometric measures. Carraro & Munari (2004) obtained CCD $UBVRI$ photometry of approximately 300 stars down to $V = 19$ mag. They found a high differential reddening across the cluster face, with an A_V which amounts to 5 mag and determined a distance of about 3.0 kpc from the Sun, found assuming an anomalous extinction law with $R_V = 3.8$ (Carraro et al. 2013).

Finally, Sher 1 is a young open cluster (10^7 years), located at $l = 289\overset{\circ}{.}64$, $b = -0\overset{\circ}{.}24$. It covers a small area of roughly $1' \times 1'$, in a distant part of the Carina arm at about 5.2 kpc from the Sun. It was investigated by Miller (1973), Moffat & Vogt (1975), and Moffat, Shara, & Potter (1991). The C-M diagram of Sher 1 indicates the presence of variable reddening across the cluster, with a mean value $E_{B-V} = 1.38$. The authors also identified a subgroup of mid-early type stars at a distance of 1.9 kpc and affected by a nearly constant interstellar reddening with $E_{B-V} = 0.49$. The cluster has a Wolf-Rayet member and an early-type B hypergiant, a potential luminous blue variable (LBV) candidate.

Membership determination using polarimetric tools is a productive task, (e.g., Orsatti, Vega, & Marraco 2000), but several investigations have recently determined them for these clusters, so we will concentrate on the identification of stars with signatures of intrinsic polarization, in order to compare their number with those in other clusters associated to HII regions (e.g., in NGC 6611, IC 2944); we will also study the dust distribution in the direction of the clusters, and analyze if there are polarimetric evidences on the existence (or not) of an abnormal reddening in both NGC 3603 and Westerlund 2.

2. OBSERVATIONS

Observations of the $UBV(RI)_{\rm KC}$ bands (KC: Kron-Cousins, $\lambda_{U_{\rm eff}}$=0.36 μm, FWHM=0.05 μm; $\lambda_{B_{\rm eff}}$=0.44 μm, FWHM=0.06 μm; $\lambda_{V_{\rm eff}}$=0.53 μm, FWHM=0.06 μm; $\lambda_{R_{\rm eff}}$=0.69 μm, FWHM=0.18 μm; $\lambda_{I_{\rm eff}}$=0.83 μm, FWHM=0.15 μm) were carried out using the five-channel photopolarimeter of the Torino Astronomical Observatory (FOTOR) attached to the 2.15 m telescope at the Complejo Astronómico El Leoncito (San Juan, Argentina). The instrument allows simultaneous polarization measurements to be performed in the five bands $UBVRI$, and the combination of the dichroic beam splitters and the filters cemented to the field lenses of the dichroic filters set closely matches the stan-

TABLE 1

OBSERVED STARS OF NGC 3603, WESTERLUND 2 AND SHER 1

Identification			Coordinates		Diaph. Ap.	Identification		Coordinates		Diaph. Ap.
Star[a]	MTT[c]	POS[c]	R.A.(2000)	Dec.(2000)	arcsec	Star[b]	MV[c]	R.A.(2000)	Dec.(2000)	arcsec
3603-1			11:15:05.9	−61:13:56.9	11	West2-18	5	10:24:02.4	−57:44:36.5	11
-2	20		11:15:12.9	−61:14 11.3	11	-91	3	10:24:02.2	−57:45:03.4	11
-3	2		11:15:24.0	−61:15:01.0	11	-101		10:23:57.2	−57:44:37.0	5.5
-4	71	202	11:15:21.3	−61:15:04.4	7.7	-123		10:23:56.8	−57:45:13.9	7.7
-6			11:15:27.9	−61:15:50.7	7.7	-130		10:24:02.4	−57:45:15.0	7.7
-7	27		11:15:16.8	−61:16:44.5	7.7	-158	1	10:23:59.6	−57:45:23.0	11
-8			11:15:21.1	−61:17:05.1	11	-165		10:23:55.3	−57:45:51.0	7.7
-9			11:15:15.3	−61:17:33.8	11	-171		10:24:04.9	−57:46:01.9	11
-11			11:15:15.0	−61:17:48.3	11	-182		10:23:56.2	−57:45:29.9	11
-12			11:15:15.4	−61:17:57.1	11	-240	4	10:23:58.1	−57:45:49.0	11
-13			11:15:33.9	−61:18:19.1	11	-249		10:23:59.3	−57:45:51.0	7.7
-14			11:15:26.9	−61:17:48.0	11	-263		10:24:01.5	−57:45:56.9	7.7
-15			11:15:25.5	−61:18 03.2	11	-273	8	10:23:52.7	−57:46:01.9	11
-17	34	186	11:14:55.3	−61:15:20.7	7.7	Sher1-77		11:01:06.2	−60:14:33.9	11
-18	29	64	11:15:09.1	−61:15:59.8	5.5	-82		11:01:05.7	−60:13:47.5	15.4
-19	19	74	11:15:11.3	−61:15:55.6	5.5	-106		11:01:04.1	−60:14:18.7	7.7
-20	49	103	11:15:11.1	−61:15:36.8	5.5	-122		11:01:02.9	−60:13:56.3	7.7
-21	47		11:15:11.1	−61:15:36.8	5.5	-125		11:01:02.7	−60:15:16.5	11
-22	18		11:15:10.1	−61:15:38.2	5.5	-139		11:01:01.6	−60:13:48.8	11
-23	12	157	11:15:09.8	−61:15:30.5	5.5	-156		11:01:00.9	−60:13:55.1	7.7
-24	32	166	11:15:08.9	−61:15:27.3	5.5	-164		11:00:53.7	−60:14:31.2	11
-25	13	190	11:15:07.8	−61:15:16.7	7.7	-218		11:00:53.7	−60:13:14.6	11
-28	16	164	11:15:02.0	−61:15:28.0	7.7					
-30	7		11:15:02.6	−61:15:40.7	7.7					
-47	11	61	11:15:09.3	−61:16:02.1	5.5					
-49	41	147	11 15:09.1	−61:15:33.2	5.5					

[a]Identifications from Sher (1965).
[b]Identifications from Moffat et al. (1991).
[c]MTT: Melnick et al. (1989); MV: Moffat & Vogt (1975); POS: Pandey et al. (2000).

dard $UBVRI$ system. FOTOR offers 5 diaphragms for polarimetric use, which in combination with the 2.15 m telescope result in apertures of 5.5, 7.7, 11.0, 15.4 and 18.7 arcsecs. For additional information about the instrument, data acquisition, and data reduction, we refer to Scaltriti et al. (1989) and Scaltriti (1994). Standard stars from Turnshek et al. (1990) and from Hsu & Breger (1982) for null polarization and for the zero point of the polarization position, were observed several times each night for calibration purposes. Table 1 lists targets, their equatorial coordinates and the diaphragms used in the observation of each star.

3. RESULTS

The polarimetric observations of 28 stars in the direction of NGC 3603 was performed in the years 1998 to 2001. They are listed in Table 2 which shows, in self-explanatory format, the stellar identification as given by Sher (1965), the percentage polarization (P_λ), the position angle of the electric vector (θ_λ) in the equatorial coordinate system, and their respective mean errors for each filter, computed considering the photon shot noise as the dominant source of errors (Maronna, Feinstein, & Clocchiatti 1992). Additional identifications from Melnick et al. (1989) are also provided.

A few stars in the directions of Westerlund 2 and of Sher 1 were observed with lower accuracy (13 and 9 stars, respectively) due to the high concentration to the center of the clusters and because of background contamination. The observations of both sets of objects were made in the years 2000 to 2005 in common with other projects, and Table 3 shows the polarimetric observations of these stars with the format of Table 2. The stellar identifications are taken from Moffat et al. (1991), additional identifications for Westerlund 2 from Moffat & Vogt (1975).

4. ANALYSIS AND DISCUSSION

4.1. *Fitting with Serkowski's law*

To analyze the data, the polarimetric observations in the five filters were fitted for each star using Serkowski's law of interstellar polarization (Serkowski 1973) given by

$$P_\lambda/P_{\lambda_{\max}} = e^{-K\ln^2(\lambda_{\max}/\lambda)}\,. \qquad (1)$$

TABLE 2

POLARIMETRIC OBSERVATIONS IN THE OPEN CLUSTER NGC 3603

Star[a]	Id[b]	Filter	$P_\lambda \pm \epsilon_P$ (%)	$\theta_\lambda \pm \epsilon_\theta$ (°)	Star[a]	Id[b]	Filter	$P_\lambda \pm \epsilon_P$ (%)	$\theta_\lambda \pm \epsilon_\theta$ (°)
1		*U*	2.88 ± 1.17	60.0 ± 11.1	17*	MTT34	*U*	2.88 ± 1.17	117.9 ± 11.0
		B	1.80 ± 0.33	86.5 ± 5.3			*B*	2.86 ± 0.76	116.8 ± 7.5
		V	1.25 ± 0.07	83.3 ± 1.5			*V*	1.93 ± 0.13	109.8 ± 1.9
		R	1.38 ± 0.06	81.6 ± 1.2			*R*	2.23 ± 0.16	111.7 ± 2.0
		I	1.10 ± 0.11	76.9 ± 2.8			*I*	2.18 ± 0.22	109.9 ± 2.9
2	MTT20	*U*	0.85 ± 0.34	60.7 ± 10.9	18*	MTT14	*U*	1.25 ± 0.32	98.7 ± 7.2
		B	0.74 ± 0.18	78.4 ± 6.9			*B*	0.69 ± 0.27	115.3 ± 10.6
		V	0.79 ± 0.05	78.0 ± 1.9			*V*	0.85 ± 0.21	122.3 ± 7.1
		R	0.77 ± 0.05	83.6 ± 2.0			*R*	0.97 ± 0.24	115.4 ± 6.9
		I	0.93 ± 0.12	83.9 ± 3.5			*I*	0.90 ± 0.25	121.5 ± 7.8
3	MTT2	*U*	0.65 ± 0.16	77.0 ± 7.0	19*	MTT25	*U*	0.68 ± 0.41	166.1 ± 15.7
		B	0.64 ± 0.07	73.3 ± 3.1			*B*	0.83 ± 0.29	141.1 ± 9.6
		V	0.72 ± 0.03	83.1 ± 1.3			*V*	0.79 ± 0.14	138.5 ± 5.0
		R	0.70 ± 0.05	79.5 ± 2.1			*R*	0.59 ± 0.14	141.3 ± 6.8
		I	0.70 ± 0.09	78.8 ± 3.5			*I*	0.90 ± 0.21	142.9 ± 6.5
4	MTT71	*U*	7.70 ± 3.53	75.8 ± 12.3	20*	MTT49	*U*	2.57 ± 0.94	171.1 ± 10.1
		B	3.84 ± 0.40	110.2 ± 3.0			*B*	3.41 ± 0.30	119.8 ± 2.5
		V	5.15 ± 0.13	104.7 ± 0.7			*V*	2.19 ± 0.23	128.2 ± 3.0
		R	5.32 ± 0.21	104.9 ± 1.1			*R*	1.74 ± 0.13	122.0 ± 2.1
		I	4.63 ± 0.22	102.8 ± 1.3			*I*	1.73 ± 0.18	130.6 ± 3.1
6		*U*	2.42 ± 1.21	106.2 ± 13.3	21*	MTT47	*U*	4.36 ± 1.28	114.6 ± 8.2
		B	4.94 ± 0.50	116.6 ± 2.9			*B*	1.83 ± 0.48	140.3 ± 7.3
		V	4.31 ± 0.10	103.9 ± 0.7			*V*	2.10 ± 0.42	109.1 ± 5.7
		R	4.33 ± 0.07	107.8 ± 0.5			*R*	2.04 ± 0.49	117.8 ± 6.8
		I	3.95 ± 0.14	105.3 ± 1.0			*I*	1.72 ± 0.36	126.7 ± 5.9
7	MTT27	*U*	2.57 ± 1.05	111.5 ± 11.1	22*	MTT18	*U*	1.98 ± 0.51	122.7 ± 7.2
		B	0.09 ± 0.32	82.5 ± 37.3			*B*	2.00 ± 0.19	128.6 ± 2.7
		V	0.55 ± 0.21	50.7 ± 10.4			*V*	2.37 ± 0.13	128.2 ± 1.6
		R	0.50 ± 0.13	63.4 ± 7.2			*R*	2.27 ± 0.06	129.5 ± 0.7
		I	0.49 ± 0.50	165.2 ± 22.9			*I*	2.07 ± 0.04	128.4 ± 0.5
8		*U*	1.07 ± 1.46	158.9 ± 26.9	23*	MTT12	*U*	1.36 ± 0.35	126.3 ± 7.2
		B	0.80 ± 0.29	62.7 ± 9.9			*B*	1.97 ± 0.17	130.4 ± 2.5
		V	0.15 ± 0.10	91.4 ± 16.6			*V*	1.85 ± 0.09	128.4 ± 1.4
		R	0.43 ± 0.06	85.8 ± 4.0			*R*	2.12 ± 0.10	129.9 ± 1.3
		I	0.34 ± 0.08	81.4 ± 6.6			*I*	1.67 ± 0.08	132.8 ± 1.4
9		*U*	1.36 ± 0.36	41.6 ± 7.5	24*	MTT32	*U*	1.57 ± 0.66	174.9 ± 11.3
		B	0.46 ± 0.13	61.2 ± 7.7			*B*	1.89 ± 0.43	127.3 ± 6.4
		V	0.41 ± 0.13	70.9 ± 9.1			*V*	1.65 ± 0.33	133.9 ± 5.7
		R	0.42 ± 0.09	68.3 ± 5.9			*R*	2.10 ± 0.29	135.7 ± 3.9
		I	0.54 ± 0.19	65.5 ± 9.1			*I*	1.91 ± 0.28	143.8 ± 5.0
10		*U*	2.25 ± 1.80	43.0 ± 19.3	25*	MTT13	*U*	3.64 ± 0.44	104.4 ± 3.5
		B	0.61 ± 0.37	74.0 ± 15.4			*B*	3.86 ± 0.18	115.0 ± 1.3
		V	1.85 ± 0.31	80.9 ± 4.7			*V*	3.51 ± 0.09	112.4 ± 0.8
		R	1.11 ± 0.18	86.3 ± 4.6			*R*	3.12 ± 0.08	112.9 ± 0.3
		I	1.52 ± 0.43	77.8 ± 8.0			*I*	2.79 ± 0.06	114.1 ± 0.6
11		*U*	0.65 ± 0.57	116.2 ± 20.7	26	MTT35	*U*	1.50 ± 1.62	38.8 ± 23.6
		B	1.68 ± 0.38	96.1 ± 6.3			*B*	2.03 ± 1.13	150.9 ± 14.6
		V	0.99 ± 0.27	109.8 ± 7.6			*V*	1.11 ± 0.15	110.9 ± 9.6
		R	0.66 ± 0.33	124.0 ± 13.4			*R*	0.87 ± 0.24	103.3 ± 11.8
		I	0.63 ± 0.40	112.0 ± 16.3			*I*	1.02 ± 0.28	145.2 ± 17.1
12		*U*	10.47 ± 3.98	151.9 ± 10.4	28	MTT16	*U*	1.01 ± 0.49	67.7 ± 12.8
		B	1.85 ± 0.77	137.4 ± 11.3			*B*	0.91 ± 0.50	71.7 ± 14.4
		V	0.78 ± 0.86	97.3 ± 23.8			*V*	1.42 ± 0.17	58.2 ± 3.3
		R	1.67 ± 0.79	67.9 ± 12.6			*R*	1.22 ± 0.19	50.6 ± 4.4
		I	2.23 ± 1.65	147.9 ± 18.3			*I*	1.27 ± 0.35	51.2 ± 7.9
13		*U*	0.65 ± 0.13	69.0 ± 5.8	30	MTT7	*U*	0.52 ± 0.19	73.0 ± 10.2
		B	0.57 ± 0.09	72.4 ± 2.2			*B*	0.46 ± 0.19	69.2 ± 11.1
		V	0.59 ± 0.08	70.3 ± 0.8			*V*	0.50 ± 0.07	19.3 ± 4.0
		R	0.60 ± 0.09	70.1 ± 0.6			*R*	0.45 ± 0.07	17.1 ± 4.5
		I	0.55 ± 0.07	68.1 ± 1.4			*I*	0.52 ± 0.13	18.5 ± 7.2
14		*U*	0.55 ± 0.11	80.8 ± 5.7	47*	MTT11	*U*	1.79 ± 0.54	129.2 ± 8.4
		B	0.62 ± 0.06	88.9 ± 2.8			*B*	1.96 ± 0.30	127.9 ± 4.4
		V	0.59 ± 0.04	94.0 ± 1.9			*V*	2.04 ± 0.18	116.1 ± 2.5
		R	0.58 ± 0.04	92.9 ± 2.0			*R*	1.76 ± 0.15	120.7 ± 2.5
		I	0.42 ± 0.09	99.6 ± 6.4			*I*	1.68 ± 0.24	118.3 ± 4.0
15		*U*	0.56 ± 0.22	60.9 ± 10.7	49*	MTT41	*U*	0.94 ± 1.09	90.2 ± 24.7
		B	0.95 ± 0.14	80.1 ± 4.3			*B*	0.81 ± 1.02	91.9 ± 25.8
		V	0.92 ± 0.07	84.5 ± 2.1			*V*	1.41 ± 0.22	136.8 ± 4.4
		R	0.82 ± 0.09	82.6 ± 3.3			*R*	1.10 ± 0.15	135.2 ± 3.9
		I	0.86 ± 0.23	87.6 ± 7.4			*I*	1.02 ± 0.28	145.2 ± 17.1

[a]Identifications from Sher (1965); * stands for member.
[b]Identifications from Melnick et al. (1989).

TABLE 3

POLARIMETRIC OBSERVATIONS IN THE OPEN CLUSTERS WESTERLUND 2 AND SHER 1

Star[a]	Id[b]	Filter	$P_\lambda \pm \epsilon_P$ (%)	$\theta_\lambda \pm \epsilon_\theta$ (°)	Star[a]	Id[b]	Filter	$P_\lambda \pm \epsilon_P$ (%)	$\theta_\lambda \pm \epsilon_\theta$ (°)
West2-18*	MV5	U	– –	– –	West2-263*		U	– –	– –
		B	3.74 ± 0.18	109.7 ± 1.4			B	5.20 ± 0.71	147.2 ± 3.9
		V	4.39 ± 0.12	104.3 ± 0.8			V	5.07 ± 0.16	124.4 ± 0.9
		R	4.50 ± 0.11	106.1 ± 0.7			R	6.46 ± 0.15	139.9 ± 0.7
		I	4.14 ± 0.68	106.4 ± 0.5			I	5.03 ± 0.12	132.7 ± 0.5
West2-91	MV3	U	– –	– –	West2-273	MV8	U	– –	– –
		B	1.62 ± 0.23	171.5 ± 4.1			B	– –	– –
		V	3.32 ± 0.43	175.1 ± 3.7			V	1.53 ± 0.13	138.2 ± 2.4
		R	2.50 ± 0.34	172.8 ± 3.9			R	1.55 ± 0.11	138.0 ± 2.0
		I	3.67 ± 0.65	178.2 ± 5.1			I	1.50 ± 0.19	128.4 ± 3.7
West2-101*		U	– –	– –	Sher1-77	MV5	U	1.53 ± 0.23	99.7 ± 4.2
		B	– –	– –			B	0.52 ± 0.37	81.6 ± 17.5
		V	3.19 ± 0.42	102.9 ± 5.3			V	0.66 ± 0.19	123.5 ± 8.0
		R	3.34 ± 0.40	111.8 ± 5.6			R	0.97 ± 0.17	122.3 ± 5.0
		I	3.89 ± 0.39	105.1 ± 3.2			I	0.61 ± 0.60	128.0 ± 22.2
West2-123*		U	– –	– –	Sher1-82	MV1	U	1.16 ± 0.21	61.8 ± 5.1
		B	– –	– –			B	1.06 ± 0.03	88.3 ± 0.7
		V	5.32 ± 0.31	108.4 ± 0.7			V	1.08 ± 0.05	91.0 ± 1.4
		R	4.91 ± 0.23	109.8 ± 0.4			R	1.05 ± 0.02	88.3 ± 0.5
		I	4.95 ± 0.39	116.4 ± 0.6			I	0.81 ± 0.04	88.9 ± 1.5
West2-130*		U	– –	– –	Sher1-106*	MV6	U	6.36 ± 1.77	6.0 ± 7.8
		B	– –	– –			B	5.53 ± 0.69	24.3 ± 3.0
		V	4.89 ± 0.53	178.9 ± 8.7			V	3.42 ± 0.25	27.3 ± 2.1
		R	4.60 ± 0.33	174.4 ± 10.4			R	3.51 ± 0.16	28.0 ± 2.8
		I	5.01 ± 0.61	173.1 ± 10.5			I	2.69 ± 0.28	26.6 ± 3.0
West2-158	MV1	U	– –	– –	Sher1-122*	MV2	U	1.84 ± 1.08	36.3 ± 15.2
		B	– –	– –			B	2.76 ± 0.14	25.3 ± 1.5
		V	3.29 ± 0.50	111.6 ± 6.1			V	2.54 ± 0.15	22.9 ± 1.7
		R	4.46 ± 0.44	113.3 ± 2.8			R	2.70 ± 0.21	27.7 ± 2.2
		I	3.16 ± 0.44	104.4 ± 5.4			I	2.47 ± 0.21	27.8 ± 2.5
West2-165*		U	– –	– –	Sher1-125		U	0.38 ± 0.14	115.2 ± 10.0
		B	– –	– –			B	0.94 ± 0.12	96.7 ± 3.6
		V	3.79 ± 0.43	116.5 ± 2.9			V	0.61 ± 0.07	94.5 ± 3.2
		R	3.81 ± 0.41	103.0 ± 4.9			R	0.61 ± 0.08	93.7 ± 3.7
		I	3.14 ± 0.45	117.0 ± 2.7			I	0.53 ± 0.09	87.1 ± 5.0
West2-171*		U	– –	– –	Sher1-139*	3	U	– –	– –
		B	– –	– –			B	2.35 ± 0.59	27.9 ± 7.1
		V	4.02 ± 0.24	105.5 ± 1.7			V	2.72 ± 0.23	25.9 ± 2.5
		R	5.11 ± 0.25	105.0 ± 1.4			R	2.86 ± 0.34	29.5 ± 3.4
		I	3.56 ± 0.22	104.7 ± 1.8			I	2.72 ± 0.32	29.7 ± 3.4
West2-182*		U	– –	– –	Sher1-156*		U	– –	– –
		B	– –	– –			B	– –	– –
		V	5.94 ± 0.27	111.3 ± 0.3			V	2.12 ± 0.26	45.1 ± 3.5
		R	6.19 ± 0.17	110.8 ± 0.2			R	2.50 ± 0.19	45.1 ± 2.2
		I	4.69 ± 0.12	111.8 ± 0.9			I	2.68 ± 0.25	50.5 ± 2.7
West2-240*	MV4	U	7.40 ± 0.88	95.9 ± 3.1	Sher1-164	MV4	U	1.23 ± 0.43	160.2 ± 9.7
		B	5.17 ± 0.28	97.8 ± 3.3			B	0.78 ± 0.10	100.2 ± 3.7
		V	5.16 ± 0.16	98.5 ± 0.9			V	0.95 ± 0.27	90.6 ± 8.1
		R	5.45 ± 0.12	99.5 ± 0.6			R	1.29 ± 0.31	85.1 ± 6.8
		I	5.03 ± 0.15	99.5 ± 0.8			I	1.23 ± 0.30	86.2 ± 6.9
West2-249*		U	– –	– –	Sher1-218		U	– –	– –
		B	4.23 ± 0.62	72.3 ± 3.5			B	1.01 ± 0.17	127.4 ± 4.8
		V	4.89 ± 0.38	78.6 ± 1.4			V	0.81 ± 0.10	120.6 ± 3.4
		R	5.35 ± 0.52	88.7 ± 0.9			R	0.91 ± 0.07	115.1 ± 2.3
		I	5.07 ± 0.43	82.5 ± 2.4			I	0.67 ± 0.22	99.0 ± 9.1

[a]Identifications from Moffat et al. (1991); * stands for member.
[b]Identifications from Moffat & Vogt (1975).

If polarization is produced by aligned interstellar dust particles, then we assume that the observed data (in terms of wavelength within the bands $UBVRI$) can be reproduced accurately by equation (1) and that each star has a separate $\lambda_{\rm max}$ and a $P_{\lambda_{\rm max}}$ value. To perform the fitting, we adopted

TABLE 4

POLARIZATION RESULTS OF STARS IN THE DIRECTION OF NGC 3603

Star[a]	$P_{\max} \pm \epsilon_p$ %	σ_1[b]	$\lambda_{\max} \pm \epsilon_\lambda$	Sp	E_{B-V} mag	Ref.[c]
1	1.35 ± 0.07	1.73	0.60 ± 0.07	-	0.22	1
2	0.82 ± 0.04	1.12	0.64 ± 0.08	-	0.25	1
3	0.73 ± 0.02	0.57	0.60 ± 0.03	A0	0.31	2
4	5.28 ± 0.07	0.77	0.60 ± 0.02	-	(1.39)	1
6	4.43 ± 0.08	1.23	0.60 ± 0.03	-	(1.60)	1
9	0.49 ± 0.08	1.64	0.52 ± 0.14	-	0.25	1
13	0.61 ± 0.01	0.98	0.60 ± 0.02	K2	0.35	2
14	0.61 ± 0.02	0.63	0.51 ± 0.03	-	0.30	1
15	0.91 ± 0.04	0.72	0.57 ± 0.06	-	0.35	1
17*	2.20 ± 0.14	1.23	0.70 ± 0.09	-	(1.53)	1
18*	0.97 ± 0.13	1.06	0.55 ± 0.11	O3.5 If	1.53	3
19*	0.78 ± 0.09	0.95	0.56 ± 0.12	O3 V((f))	1.35	3
20*	2.57 ± 0.63	2.14	0.40 ± 0.08	-	(1.39)	1
21*	2.16 ± 0.24	1.15	0.50 ± 0.08	O6 V((f))	1.44	3
22*	2.30 ± 0.03	0.50	0.59 ± 0.01	O3 III(f)	1.39	3
23*	1.98 ± 0.08	1.54	0.59 ± 0.04	OC9.7 Ia	1.39	3
24*	2.03 ± 0.12	0.62	0.64 ± 0.06	O6 V	1.43	3
25*	3.43 ± 0.18	2.66	0.50 ± 0.04	B1 Iab	1.60	3
28	1.34 ± 0.07	0.57	0.59 ± 0.07	-	0.30	1
30	0.51 ± 0.03	0.60	0.55 ± 0.06	-	0.21	1
47*	2.01 ± 0.06	0.41	0.52 ± 0.02	O4 V	1.47	3
49*	1.27 ± 0.14	0.91	0.56 ± 0.13	O7.5 V	1.42	3

[a]Identifications from Sher (1965); * stands for member.

[b]${\sigma_1}^2 = \sum (r_\lambda/\epsilon_{p_\lambda})^2/(m-2)$ where m is the number of colors and $r_\lambda = P_\lambda - P_{\max} \exp(-K \ln^2(\lambda_{\max}/\lambda))$.

[c]Reference: (1) calculated; (2) Cannon & Mayall (1949); (3) Melena et al. (2008).

$K = 1.66\lambda_{\max} + 0.01$, where $\lambda_{\max}$ is in μm (Whittet et al. 1992). The individual $P_{\lambda_{\max}}$, $\lambda_{\max}$, and $\bar{\epsilon}$ values are listed in Table 4 (NGC 3603) and in Table 5 (Westerlund 2 and Sher 1). Observed stars with errors in $P_{\max}$ greater than 15% were excluded from these tables. The exception is star 20, a member of the cluster with intrinsic polarization, since the $P_{\max}$ error results from its nature.

For each star, we also computed the σ_1 parameter (the unit weight error of the fit) in order to quantify the departure of our data from the "theoretical curve" of Serkowski's law. In our scheme, when a star exhibits $\sigma_1 > 1.80$ this is indicative of a partly non-interstellar origin of the measured polarization (that is, an intrinsic polarization). The dominant source of intrinsic polarization is non-spherically distributed dust and, for classical Be stars, electron scattering. The mathematical expression used to obtain the individual σ_1 values is found in both tables as a footnote. There is a second criterion to test for intrinsic polarization in the light from a star, through the $\lambda_{\max}$ values: stars with a $\lambda_{\max}$ much shorter than the average value for the interstellar medium (0.55 μm; Serkowski, Mathewson, & Ford 1975) are also likely to contain an intrinsic component of polarization (Orsatti, Vega, & Marraco 1998). Both Tables 4 and 5 also list spectral types, excesses, and their references. In the few cases where no spectra were found in the literature, individual dereddening was carried out using the relation of Schmidt-Kaler (1982) to the ZAMS relation in the color-color plot, using UBV observations listed in the WEBDA database. This method takes the star as being of luminosity class V; for non-members stars located between Sun and cluster, the calculated excesses will be fairly good, but for stars at the cluster distance

TABLE 5

POLARIZATION RESULTS OF STARS IN THE DIRECTIONS OF WESTERLUND 2 AND SHER 1

Star[a]	$P_{\max} \pm \epsilon_p$ %	σ_1[b]	$\lambda_{\max} \pm \epsilon_\lambda$	Sp	E_{B-V} mag	Ref.[c]
West2-18*	4.54 ± 0.05	0.49	0.65 ± 0.01	O3 III((f)	1.65	1
West2-91	3.21 ± 1.10	2.04	0.92 ± 0.23	G0 V-III	0.09	2
West2-101*	3.72 ± 0.30	0.90	0.80 ± 0.11	–	(1.52)	3
West2-123*	5.24 ± 0.28	1.33	0.60 ± 0.07	–	(1.44)	3
West2-130*	4.86 ± 0.31	1.17	0.65 ± 0.12	–	(1.47)	3
West2-158	3.77 ± 0.52	1.90	0.64 ± 0.21	G8 III	0.22	4
West2-165*	3.87 ± 0.16	0.42	0.56 ± 0.04	O4 V	1.80	5
West2-171*	4.37 ± 0.62	3.81	0.60 ± 0.16	O3 V((f))	1.98	1
West2-182*	6.47 ± 0.99	3.41	0.50 ± 0.08	O3 V((f))	1.79	1
West2-240*	5.56 ± 0.21	2.48	0.60 ± 0.04	WN7	1.70	1
West2-249*	5.30 ± 0.02	0.08	0.69 ± 0.01	–	(1.70)	3
West2-263*	5.68 ± 0.37	4.41	0.65 ± 0.09	O3 V((f))	2.18	1
West2-273	1.58 ± 0.02	0.29	0.64 ± 0.03	–	0.30	3
Sher1-77	1.04 ± 0.32	1.91	0.42 ± 0.15	A2 V	0.32	2
Sher1-82	1.11 ± 0.03	1.46	0.52 ± 0.02	B4 V-III	0.23	2
Sher1-106*	3.92 ± 0.48	2.03	0.48 ± 0.07	B1:Iab:	1.24	2
Sher1-122*	2.80 ± 0.11	1.20	0.57 ± 0.04	B1:Ia+e	1.34	2
Sher1-125	0.65 ± 0.07	1.72	0.55 ± 0.10	–	0.52	3
Sher1-139*	2.88 ± 0.01	0.04	0.66 ± 0.00	O8:Iab	1.40	2
Sher1-156*	2.64 ± 0.06	0.28	0.83 ± 0.03	–	(1.53)	3
Sher1-164	1.20 ± 0.17	0.92	0.77 ± 0.14	G2 V-III	0.22	2
Sher1-218	0.92 ± 0.07	1.09	0.56 ± 0.09	–	0.46	3

[a]Identifications from Sher (1965); * stands for member.

[b]${\sigma_1}^2 = \sum (r_\lambda/\epsilon_{p\lambda})^2/(m-2)$ where m is the number of colors and $r_\lambda = P_\lambda - P_{\max} \exp(-K \ln^2(\lambda_{\max}/\lambda))$.

[c]Reference: (1) Carraro et al. (2013); (2) Moffat et al. (1991); (3) calculated excess; (4) Rauw et al. (2011); (5) Vargas Alvarez et al. (2013).

or at larger distances they could be wrong. For this reason, we show some excesses between brackets in Tables 4 and 5. For the two stars with classification given by Cannon & Mayall (1949), a luminosity class V was adopted.

NGC 3603: In Table 4, three stars exhibit signatures of intrinsic polarization using the first criterion, that of the σ_1 value as an indicator: they are numbers 1, 20 and 25. The second criterion did not provide other stars. Star 1 has a σ_1 value slightly below the adopted limit of 1.80, but as this limit is indicative only and resulted from our general experience, we decided to include it in the analysis. Star 25 (B1 Iab) has a color excess larger than average; it has been compared to the progenitor of SN 1987A (Smith 2007; Smartt et al. 2002) and has detectable circumstellar material (Brandner et al. 1997). In Figure 1, the P_λ values do not fit the Serkowski's law in the filters U and B. Star 1 has similar spectral type (B1.5 Iab) and plots, so we think there is circumstellar material also in this case.

Westerlund 2: In Table 5, we find six stars with signatures of intrinsic polarization. Two of them are non-members (91 and 158) with spectral types G0 V-III y G0 III respectively; we associate the intrinsic polarization with their evolutive states. The rest are cluster members: numbers 171 (O5V), 182 (O4V-III), 240 (WN7) and 263 (O6.5V). Rauw, Sana, & Nazé (2011) studied eclipsing binaries in the core of Westerlund 2, in order to constrain the cluster distance. They included in the analysis three of our stars as binary candidates: stars 18, 171 and 182;

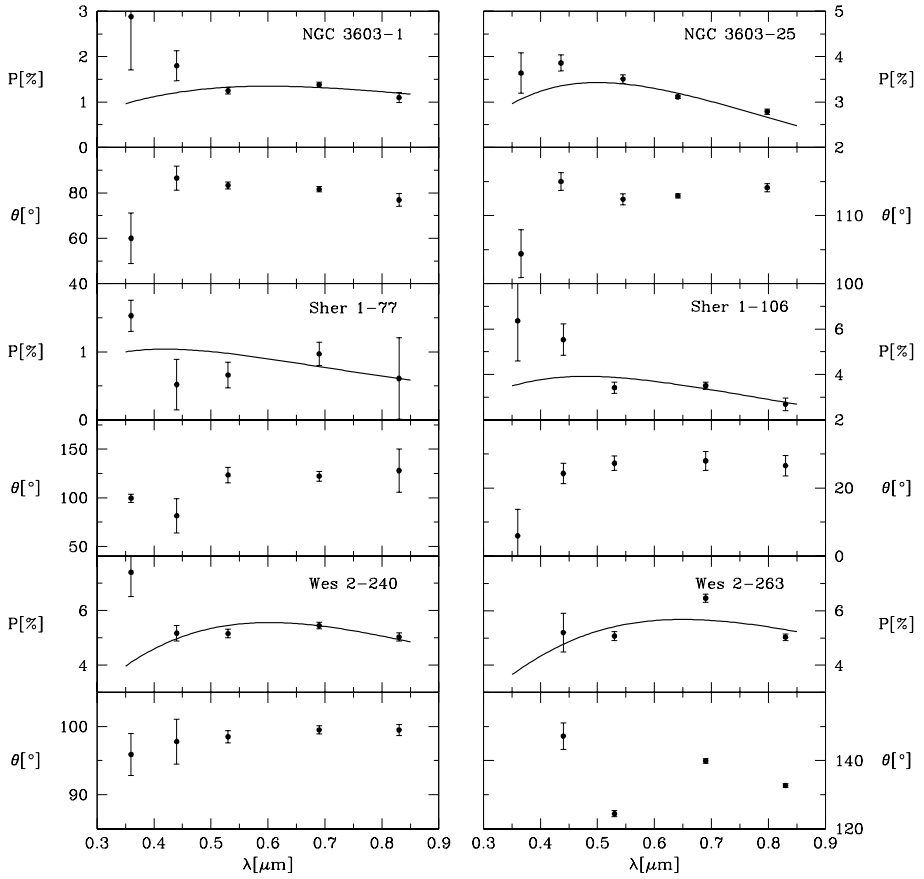

Fig. 1. Polarization and position angle dependence on wavelength, for some of the stars with indications of intrinsic polarization in NGC 3603, Westerlund 2 and Sher 1.

and assuming that there is a prevalence of short-orbital period systems, they concluded that none of them displayed significant radial velocity variations on timescales of a week. On them, number 18, has a low σ_1 (0.49); the situation of stars 171 and 182 (high $\sigma_1$values of 3,81 and 3.41 respectively) is different. Not being able to find other possible origin for such high values of the parameter, we think that the two stars may be part of binary systems, with orbital periods longer than those investigated by Rauw et al. (2011).

Sher 1: Two stars show indications of intrinsic polarization in Table 5: star 77 ($\sigma_1 = 1.91$; A2 V) and star 106 ($\sigma_1 = 2.03$; B1:Iab:). Plots showing the polarization and position angle dependence on wavelength for both stars are shown in Figure 1, where similarities between Sher 1-106 and NGC 3603-1 can be seen; both of them are supergiants. We could not find any suitable explanation for the origin of the intrinsic polarization of star 77, and we think it may be an undetected variable star.

4.2. *Polarization efficiency*

The ratio P_V/E_{B-V} is known as the polarization efficiency of the interstellar medium and it depends mainly on the alignment efficiency, the magnetic field strength and the depolarization due to radiation traversing more than one dust cloud with different field directions. If we assume normal interstellar material characterized by $R_V = 3.1$, the empirical upper limit relation for the polarization efficiency is given by:

$$P_V \leq 3\ A_V \simeq 3\ R_V\ E_{B-V}\,, \qquad (2)$$

obtained for interstellar dust particles Hiltner (1956).

NGC 3603: Figure 2 shows the relationship between the polarization P_V produced by the dust along the line of sight, and the color excess E_{B-V} for the observed stars in the direction of NGC 3603. Excesses were obtained either from the literature, or by dereddening the colors and using the relationship between spectral type and color indexes (Schmidt-

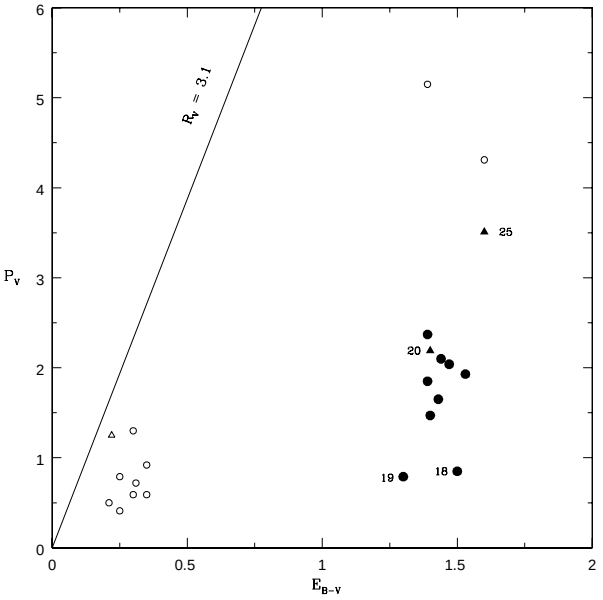

Fig. 2. Polarization efficiency diagram P_V vs. E_{B-V} for stars in the direction of NGC 3603. Filled and open circles denote members and non-members respectively; triangles, stars with intrinsic polarization according to Table 2. The line of the empirical maximum efficiency $P_V = 9.3\ E_{B-V}$ (solid line) is drawn adopting $R_V = 3.1$.

Kaler 1982). The solid line depicts this relation assuming normal interstellar material characterized by $R_V = 3.1$. The first conclusion is that, as the entire set of observed stars lies on the right of the interstellar maximum efficiency line, the observed polarization is mostly due to the ISM. We clearly identify two concentrations: one of them composed of non-member stars in the vicinity of the Sun, with excesses below 0.40 mag and polarizations under 1% (open circles); and another concentration with higher E_{B-V} values, which we associate with members (filled circles). Triangles in the plot indicate stars with intrinsic polarization.

The members show a certain dispersion in polarization values, which run from 1.40% to 2.40% approximately, due to uneven intracluster dust distribution. Stars 18 and 19 are the exception and we will comment on them. To calculate the polarization efficiency, we used 7 member stars, excluding stars 18, 19, 20 y 25. We obtained a mean efficiency $P_V/E_{B-V} = 1.34$ which is smaller than the value given by Serkowski et al. (1975), of about 5 for the interstellar medium. This depolarization can be the result of the superposition of several dust clouds in the line of sight, with different magnetic field directions.

Stars 18 and 19 (O3.5 If and O3 V ((f)) respectively; Melena et al. 2008) are cluster members according to the literature but their measured P_V are lower than for the rest. The first one displays individual P_λ values somewhat irregular which may mask an intrinsic polarization and if this is so, the actual location of star 18 in Figure 2 would be nearer to the members group. For the second, the answer could be either of two possibilities: the star is located just in front of the dust associated to the cluster or we face a situation in which the polarization efficiency amounts to 0 (because the magnetic field would be along the line of sight to the cluster) between the non-members and star 19, reaching after that a maximum efficiency (with the magnetic field on the plane of the sky, normal to the line of sight).

Westerlund 2: Figure 3 (left panel) shows that there is only one foreground star in the observed set (star 273). The important group of ten stars to the right of the plot are cluster members. Polarization and excesses show important differences, in particular in the P_V percentages (3.20% to about 5.25%), while the excesses take values between 1.30 and 1.80 mag. This is consequence of an irregular dust distribution not only across the cluster face, but also internally. The mean polarization efficiency amounts to $P_V/E_{B-V} = 2.64$.

Sher 1: In Figure 3 (right panel) we show a group of five stars located in the vicinity of the Sun (numbers 77, 82, 125, 164 and 218) which are evident non-members, with excesses E_{B-V} below 0.5 mag and polarizations P_V up to 1.25%. Another four stars (106, 122, 139, and 156) with higher polarizations (2 to 3%) and excesses around 1.5 mag, are cluster members. The polarization efficiency changes from 4.5 for the stars in the vicinity of the Sun (a value close to the average for the interstellar medium), to about 1.90 for member stars, due most probably to the existence of different clouds in the way of the light from Sher 1 (5.2 kpc) to us. As usual, non-members are plotted as open circles, filled circles are for members; and stars with intrinsic polarization are identified with triangles.

It is not possible to give a representative mean value of the polarization for Sher 1 since only two members could be observed with polarimetry, because of background contamination. We can only say is that the mean P_V could be around a high value of 2.44% and the orientation of the electric vector, around 24°.5. The mean $\lambda_{\max}$ amounts to 0.60 μm, slightly above the value of 0.55 μm for the interstellar dust. Star 156 was not included in the calculation and it will be mentioned in the next section.

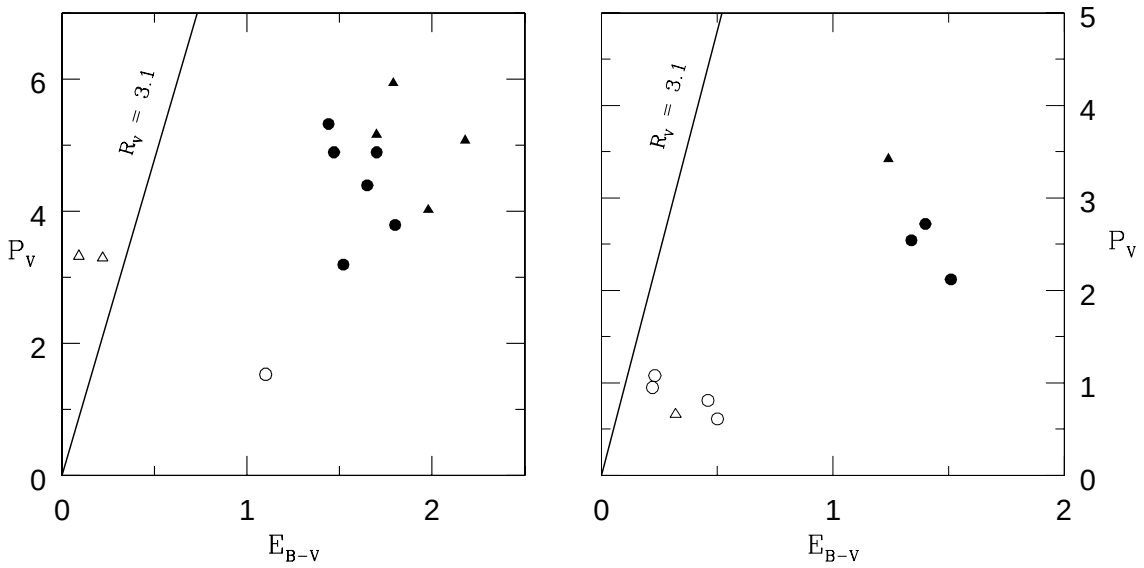

Fig. 3. Polarization efficiency diagrams for Westerlund 2 (left panel) and Sher 1 (right panel). Symbols are described in Figure 2. Triangles are used for stars with intrinsic polarization according to Table 4.

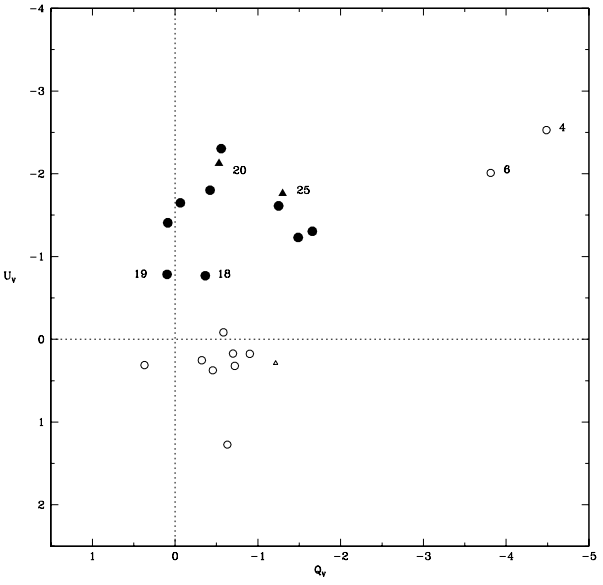

Fig. 4. Q- and U- Stokes parameters for the V bandpass of stars in NGC 3603. Filled and open circles denote members and non-members, respectively. Triangles are used for stars with intrinsic polarization according to Table 2.

4.3. *The Q_V vs. U_V plot*

The plot of the Stokes parameters Q_V versus U_V for the V-bandpass, where $Q_V = P_V \cos(2\theta_V)$ and $U_V = P_V \sin(2\theta_V)$ are the components in the equatorial system of the polarization vector P_V, is an important polarimetric tool, which illustrates the variations occurring in interstellar environments. Since the light from cluster members must have traversed a common sheet of dust of particular polarimetric characteristics, the member data points should occupy similar regions of the figure. Non-member stars (fore- and background stars) should be located in the figure somewhat apart from the region occupied by member stars, since their light must have traveled through different dust clouds from those affecting the light of member stars of different polarimetric characteristics.

NGC 3603: the plot for the observed stars is shown in Figure 4, where the point of coordinates $Q_V = 0$ and $U_V = 0$ indicates the dustless solar neighborhood, and other points represent the direction of the polarization vector P_V as seen from the Sun. There is a group of six points to the right of (0,0), which represent non-member stars in the vicinity of the Sun: they are numbers 2, 3, 9, 13, 14 and 15, under similar interstellar medium conditions ($P_V = 0.66\%$, $\theta_V = 79\overset{\circ}{.}7$; means of 6 stars each). Stars 28 and 30 are not part of that homogeneous group. The first one has a high value of the polarization compared to the rest ($P_V = 1.42\%$) and smaller θ_V ($58\overset{\circ}{.}2$); while star 30 has $P_V = 0.50\%$ which is acceptable for the group, but also has a very low θ_V ($19\overset{\circ}{.}3$). In the first case, the star may be locally affected by the irregular dust distribution; regarding the second, we think it is an undetected variable star.

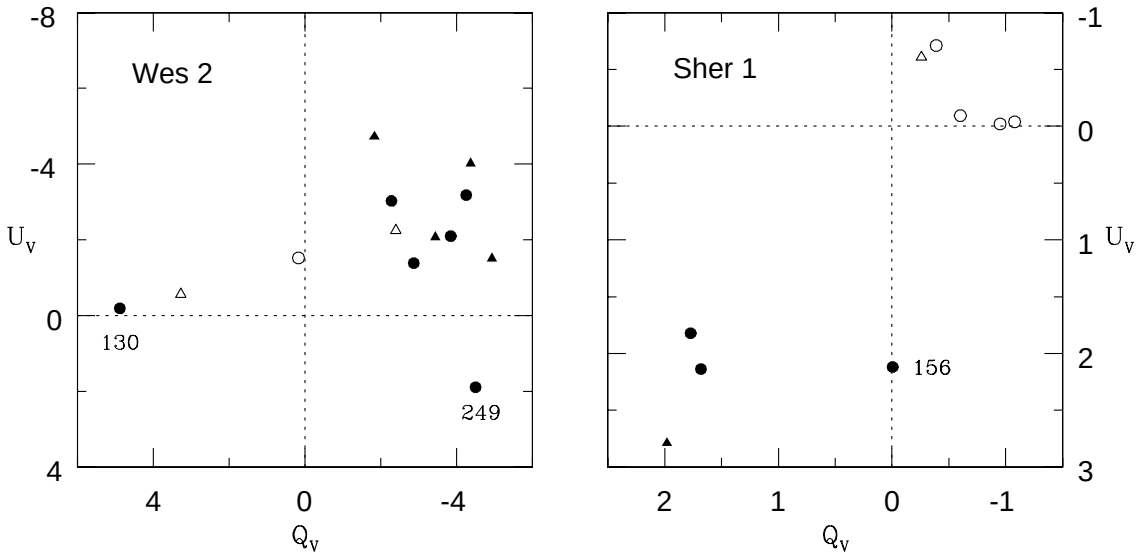

Fig. 5. Q- and U- Stokes parameters for the V bandpass of stars in the directions of Westerlund 2 (left panel) and Sher 1 (right panel). Symbols are described in Figure 2; triangles are used for stars with intrinsic polarization according to Table 4.

There are other two non-members (numbers 6 and 4) which are evident background stars. Non-members are shown with open circles.

Stars plotted with filled circles are members of NGC 3603 according to the literature. In the plane of the sky, they are distributed as having the core of the cluster at their center, and their positions in the plot show the inhomogeneity of the polarimetric characteristics in the cluster region. The mean values of polarization and orientation of the electric vector are 1.27% and 120.°0 respectively (mean of 9 each; stars with intrinsic polarization were excluded).

On the basis of this figure, we infer that there are at least two dust layers between the Sun and NGC 3603. We may characterize the first dust layer by the mean values for the group of 6 stars (recently obtained), and located at about the distance of star 3. This star has spectral type A0 V and is affected by an $E_{B-V} = 0.27$, which puts the star approximately at a distance of 0.8 kpc from the Sun. The other dust layer is in front of the cluster where, very possibly, the magnetic field orientation increases dramatically, as mentioned in another paragraph.

Westerlund 2: the plot (Figure 5, left panel) shows the concentration of members to the right, with two stars (numbers 130 and 249) identified in the literature as part of the cluster, plotted in different sections. From stars numbers 18, 101, 123, and 165 (excluding those members with intrinsic polarization), we obtained a high mean polarization $P_V = 4.11\%$ and an orientation of the electric vector $\theta_V = 108.°1$. Analyzing the position of the recently mentioned members 130 and 249, we find that the first one has $P_V = 4.89\%$ (similar to other cluster members) but a very high $\theta_V = 178.°9$. It has not been detected as having intrinsic polarization features, but considering that the σ_1 was calculated based only on three filters, we conclude the star may belong to that category. On star 249, with $P_V = 4.89\%$ and $\theta_V = 78.°6$, we think that, since only four filters to detect intrinsic polarization were used, the lack of U-filter polarization data could mask a higher than normal (in the sense of adjusting to the Serkowski's law) value. In that case, we would have scattering in an extended atmosphere, but of course this is only a supposition. In any case, if it were a member, it would have intrinsic polarization. It is not possible to give the polarimetric characteristics of the interstellar medium in the vicinity of the Sun, since we have only one non-member (star 273).

Sher 1: in the right panel of Figure 5 we show the plot for this cluster. There is a group of five non-member stars near the Sun. To calculate the characteristics of the interstellar material, we used stars 82, 125 and 164, obtaining $P_V = 0.88\%$ and $\theta_V = 91.°7$. Star 218, with a $\theta_V = 120.°0$, was not included. The small number of observed members prevents us from characterizing the interstellar material at the cluster distance (5.2 kpc) but with two stars (numbers 122 and 139) we obtain $P_V = 2.63\%$ and $\theta_V = 24.°4$,

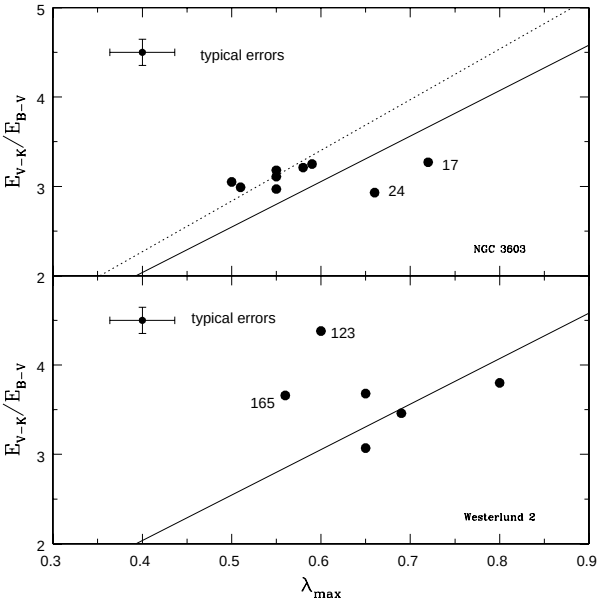

Fig. 6. E_{V-K}/E_{B-V} vs. $\lambda_{\max}$ plots for stars belonging to NGC 3603 (upper panel) and Westerlund 2 (lower panel). Stars with intrinsic polarization are not included in the plot.

which tells us that there exist a number of polarizing dust clouds along the way to the Sun, so as to change the value of the orientation of the electric vector in such way. Star 156 ($Q_V = 0$, $U_V = 2$) is member of the cluster according to the literature. In the plane of the sky it is located very close to star 139 and they have similar polarizations, but the orientation angles are very different: 45°.9 and 25°.9, respectively. A suitable explanation is that they are located right at the cluster limits and therefore not affected by the cluster magnetic field.

5. ABNORMAL REDDENING IN NGC 3603 AND WESTERLUND 2

The value of the ratio total-to-selective extinction $R_V = A_V/E_{B-V}$ is an important quantity if we want to obtain distances based on photometric data. The normal extinction law is characterized by a value $R_V = 3.1$, and a great number of investigations have found that is valid in many parts of the Galaxy. However, the studies of Neckel & Chini (1981) and of Chini & Krugel (1983) on the interstellar extinction law in HII regions associated with large amounts of gas and dust, gave evidence of abnormal R_V values in some directions of the Galaxy. Later, Tapia et al. (1988), Marraco, Vega, & Vrba (1993) and Orsatti et al. (2000) showed that the *canonical* relationship between the excesses rate E_{V-K}/E_{B-V} and $\lambda_{\max}$ is not valid for stars belonging to dusty HII regions, while this is not true for Trumpler 15, which is located well outside the HII region. The direct consequence of using a wrong R_V value is to affect the extinction-corrected magnitude and with that, the distance determination. For example, Melena et al. (2008) summarize in their Table 4 the stellar distance of NGC 3603 obtained using different values of R_V.

In order to check the *canonical* relationship between R_V and $\lambda_{\max}$ for the interstellar dust in the two HII regions connected to NGC 3603 and Westerlund 2, respectively, we plotted in Figure 6 the relationship between the excess ratio E_{V-K}/E_{B-V} and $\lambda_{\max}$ for the observed members of both open clusters. Stars suspected of having some kind of intrinsic polarization were not included. Individual K values have been obtained using the 2MASS catalogue, and the excesses E_{V-K} ratio were calculated from the relationships: $E_{V-K} = (V-K)-(V-K)_0$ where the intrinsic colors $(V-K)_0$ were taken from Tokunaga (2000).

The canonical relation E_{V-K}/E_{B-V}=5.09 $\lambda_{\max}$ (Whittet & van Breda 1978) is drawn as a solid line in both panels.

NGC 3603: the dashed line in Figure 6 (upper panel) was fitted to seven stars, obtaining:

$$E_{V-K}/E_{B-V} = 5.7\ \lambda_{\max}\,. \qquad (3)$$

As a comparison, Orsatti et al. (2000) found a value of 5.6 for the constant in equation (3) for stars in the core of NGC 6611. If we adopt $A_V/E_{V-K} = 1.12$, we get

$$R_V = 6.4\ \lambda_{\max}\,, \qquad (4)$$

compared with a *canonical* value of 5.7 for the constant in equation (4). In NGC 3603 the $\lambda_{\max}$ values that result from the observations around the central core, run from 0.50 to 0.60 μm. Adopting 0.58 μm as a mean value of $\lambda_{\max}$ for the dust in the cluster, we get an abnormal $R_V = 3.7$; we are not able to confirm if this is also true for the central core of the cluster, or if the value is even higher. Melena et al. (2008) presented in their Table 4, a list of investigations on NGC 3603 with the adopted R_V. As can be seen, many studies accepted a normal $R_V = 3.1$ or 3.2 for the observed stars in the direction of the cluster as for example Melnick et al. (1989), while others like Pandey et al. (2000) assumed a foreground reddening represented by a normal value of R for excesses up to $E_{B-V} = 1.1$, and an abnormal extinction law with $R = 4.3$ for the dust inside the cluster (excesses between 1.30 and 1.75). Even with a limited number of observations, the polarimetry favors

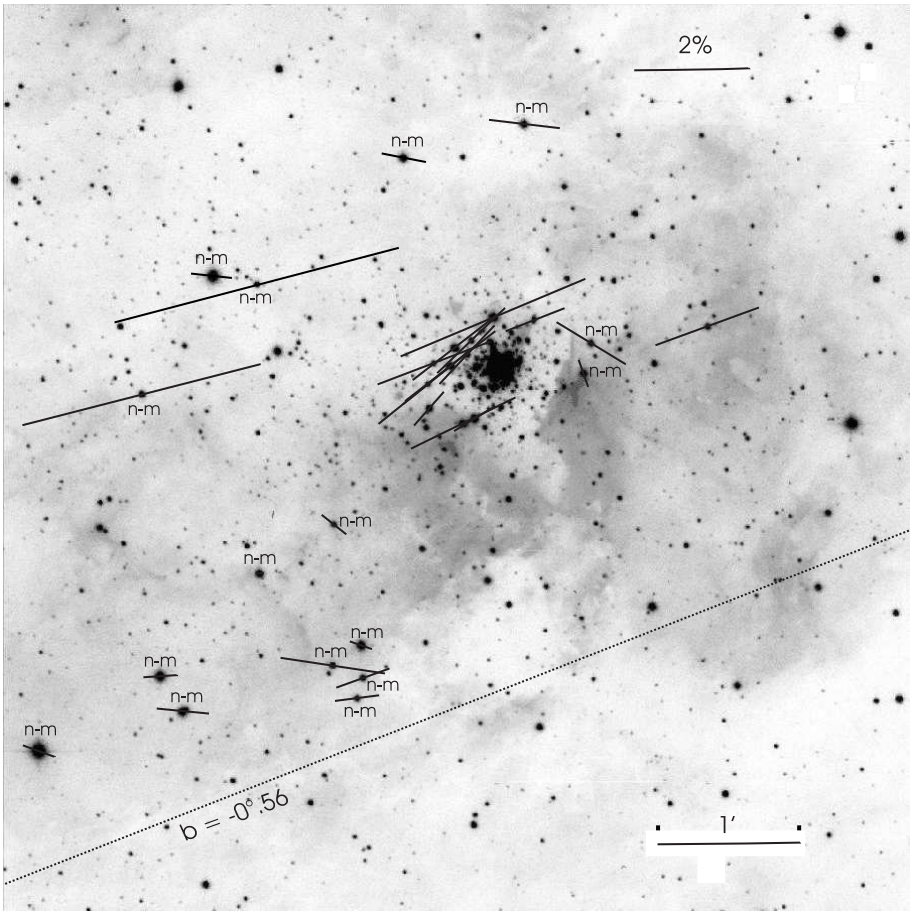

Fig. 7. Projection on the sky of the polarization vectors (Johnson V filter) of the stars observed in the region of NGC 3603; only non-member stars are identified in the figure. The dotted line is the Galactic parallel $b = -0°.56$. The length of each vector is proportional to the polarization percentage. The background image of the cluster was taken from `http://apod.nasa.gov/apod/image/0110/ngc3603_wb_big.jpg`.

the existence of an abnormal reddening, but more polarimetric observations in NGC 3603 are needed, of course.

Westerlund 2: the high percentage of stars (about 40%) with indications of intrinsic polarization leaves only six stars to be included in the plot (Figure 6, lower panel). Stars 18, 101, 130 and 249 seem to obey the canonical relation; while stars 123 and 165 are plotted well above it. If we were to fit those two points with a line, the constant in (2) would be even higher than 5.7. The mean $\lambda_{\rm max}$ for stars in this cluster is 0.65 μm, in comparison with 0.55 μm associated with the interstellar medium. Then, the parameter R_V characterizing the dust associated with Westerlund 2 could be near (or greater than) the anomalous value obtained by Carraro et al. (2013): 3.8. Again, polarimetry favors the idea of abnormal reddening in this cluster.

6. CONCLUSIONS

28 stars were observed in the direction of NGC 3603, 11 of them being members located around the central core. Three stars in the observed set display evidences of intrinsic polarization but only two of them are cluster members (one evolved star and a possible variable), a very different result when compared with the situation in NGC 6611. Polarizations for stars in the halo show a great range of values (between 1.40 and 2.40 percent), due to an uneven intracluster dust distribution. The mean particles size is only slightly larger than normal (0.58 μm vs. 0.55 μm) which could be within the errors. The dust efficiency is very low (1.34), which indicates high depolarization due to the presence of several dust clouds along the line of sight to the cluster, with different magnetic field directions. The first cloud is near the Sun with mean $P_V = 0.66$ and $\theta_V = 79.^{\circ}1$,

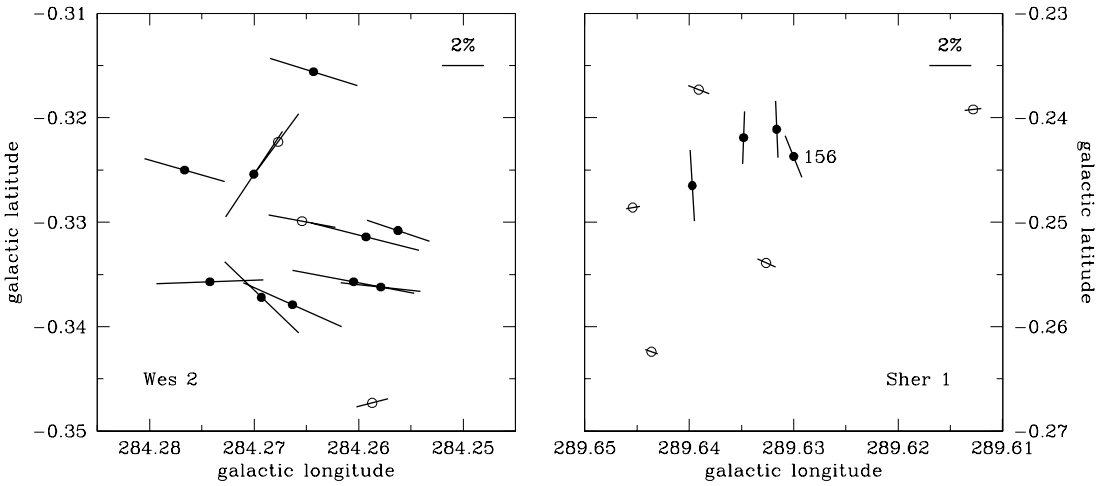

Fig. 8. Projections on the sky of the polarization vectors (Johnson V filter) of stars observed in the regions of Westerlund 2 (left panel) and Sher 1 (right panel). Filled and open circles are used for members and non-members, respectively. The length of each vector is proportional to the polarization percentage.

at about 0.8 kpc; and then there exists another slab of material just in front of the cluster as well as intracluster dust. Figure 7 shows the projection on the sky of the polarization vectors (Johnson V filter) of the stars observed in the region of NGC 3603; only non-member stars are identified in the figure. The dot-dashed line is the Galactic parallel $b = -0$. We have found through polarimetry a confirmation of anomalous reddening in NGC 3603 with an $R_V = 3.7$ in coincidence with other investigations. More polarimetric observations are required.

We observed 13 stars near the central core of Westerlund 2, two of them foreground stars. 40% of the members (6 stars) show indications of intrinsic polarization and this percentage is similar to the one found in the core of NGC 6611 and also in the study of IC 2944, both of them in HII regions. Two stars of the list are suspected members of binary systems as proposed by Rauw et al. (2011), and we regard that supposition as highly possible. We also have found another two members with intrinsic polarization according to their position in the Q vs. U plot, but this cannot be confirmed due to the lack of polarization data with some of the filters. The polarizations and excesses show important variations (3.20 to 5.3%; 1.30 to 1.80 mag respectively), due to irregular dust distribution not only across the cluster face but also internally. The mean particle size is about 0.65 μm, larger than in NGC 3603. The mean polarization efficiency is 2.64, not as small as for NGC 3603. We have only one foreground star in the vicinity of the Sun, and for this reason we cannot give information on the nearest dust cloud; but if the polarization efficiency for the light from the cluster has reached that low value it means that there must be several dust clouds in the way to Westerlund 2. The number of stars that can be used to detect anomalous reddening is very small, since stars suspected of intrinsic polarization cannot be used, but we could find indications of a value of R_V very near, or even higher, than that calculated by Carraro et al. (2013).

Finally, we observed 9 stars in the direction of Sher 1, including 4 members. We found only one member with intrinsic polarization. It is difficult to calculate a mean value of the P_V with such a small number of observed members, but we could deduce it is about 2.44%, and 0.60 μm, would be the particle size. The mean polarization efficiency is 2.64, not as small as for NGC 3603. The set of observations in the direction of the cluster includes a group of five non-member stars in the vicinity of the Sun, and for them we get an almost normal polarization efficiency of 4.5, while the value at the cluster distance is about 1.9. The first cloud is near the Sun with polarizations up to 1.25% and the recently mentioned variation in efficiency should be the result of the existence of another dust cloud, but the huge crowding of stars near the core prevented us from observing a great number of stars. Figure 8 shows the projections on the sky of the polarization vectors (Johnson V filter) of stars observed in the regions of Westerlund 2 (left panel) and Sher 1 (right panel). Filled and open circles are used for members and non-members, respectively.

As can be seen, the polarimetric tools can be very useful in the task of finding abnormal RV values in clusters suspected of presenting possible anomalous

reddening, as in NGC 3603, or at least indications of it, as in Westerlund 2. In both cases more observations are needed, to help improve the results.

We thank the referee for really improving the article. This publication makes use of data products from the Two Micron All Sky Survey, which is a joint project of the University of Massachusetts and the Infrared Processing and Analysis Center/California Institute of Technology, funded by the National Aeronautics and Space Administration and the National Science Foundation. This research has also made use of the WEBDA database, operated at the Institute for Astronomy of the University of Vienna.

We wish to acknowledge the technical support and hospitality at CASLEO during the observing runs, and the use of the Torino Photopolarimeter built at Osservatorio Astronomico di Torino (Italy) and operated under agreement between Complejo Astronómico El Leoncito and Osservatorio Astronomico di Torino. Special thanks go to Dr. Hugo G. Marraco for his useful comments and to Mrs. M. C. Fanjul de Correbo for technical assistance.

REFERENCES

Belloni, T., & Mereghetti, S. 1994, A&A, 286, 935
Brandner, W., Grebel, E. K., Chu, Y.-H., & Weis, K. 1997, ApJ, 475, L45
Cannon, A. J., & Mayall, W. M. 1949, Ann. Harvard Coll. Obs., 112, 1
Carraro, G., & Munari, U. 2004, MNRAS, 347, 625
Carraro, G., Turner, D., Majaess, D., & Baume, G. 2013, in IAU Symp. 289, Advancing the Physics of Cosmic Distances, ed. R de Grijs & G. Bono, in press (arXiv:1209.2080)
Chini, R., & Krugel, E. 1983, A&A, 117, 289
Goldwurn, A., Caraveo, P. A., & Bignami, G. F. 1987, ApJ, 322, 349
Goss, W., & Radhakrishnan, V. 1969, Astrophys. Lett., 4, 199
Hiltner, W. A. 1956, ApJS, 2, 389
Hsu, J.-C., & Breger, M. 1982, ApJ, 262, 732
Johnson, H. L. 1966, ARA&A, 4, 193
Maronna, R., Feinstein, C., & Clocchiatti, A. 1992, A&A, 260, 525
Marraco, H. G., Vega, E. I., & Vrba, F. J. 1993, AJ, 105, 258
Melena, N. W., Massey, P., Morrell, N. I., & Zangari, A. M. 2008, ApJ, 135, 878
Melnick, J., Tapia, M., & Terlevich, R. 1989, A&A, 213, 89
Miller, E. W. 1973, Bull. Am. Astron. Soc., 5, 326
Moffat, A. F. J. 1983, A&A, 124, 273
Moffat, A. F. J., Shara, M., & Potter, M. 1991, AJ, 102, 642
Moffat, A. F. J. & Vogt, N. 1975, A&AS, 20, 125
Neckel, Th., & Chini, R. 1981, A&AS, 45, 451
Orsatti, A. M., Vega, E. I., & Marraco, H. G. 1998, AJ, 116, 266
_____. 2000, A&AS, 144, 195
Pandey, A. K., Ogura, K., & Sekiguchi, K. 2000, PASP, 52, 847
Rauw, G., Sana, H., & Nazé, Y. 2011, A&A, 535, 40
Scaltriti, F. 1994, Technical Publication No. TP-001 (Turin, Italy: Obs. Astron. Torino)
Scaltriti, F., Cellino, A., Anderlucci, E., Corcione, L., & Piirola, V. 1989, Mem. Soc. Astron. Italiana, 60, 243
Schmidt-Kaler, Th. 1982, Landolt Bornstein New Series, Group VI, Vol. 2b, Stars and Stars Clusters, ed. K. Schaifers & H. H. Voigt (Berlin: Springer-Verlag)
Serkowski, K. 1973, in IAU Symp. 52, Interstellar Dust and Related Topics, ed. J. M. Greenberg & H. C. van der Hulst (Dordrecht: Reidel), 145
Serkowski, K., Mathewson, D. L., & Ford, V. L. 1975, ApJ, 196, 261
Sher, D. 1965, MNRAS, 129, 237
Smartt, S. J., Lennon, D. J., Kudritzki, R. P., Rosales, F., Ryans, R. S. I., & Wright, N. 2002, A&A, 391, 979
Smith, N. 2007, AJ, 133, 1034
Tapia, M., Roth, M., Marraco, H. G., & Ruiz, M. T. 1988, in Conference on Dust in the Universe, ed. M. E. Bailey & D. A. Williams (Cambridge: Cambridge Univ. Press), 19
Tokunaga, A. T. 2000, in Allen's Astrophysical Quantities, ed. A. N. Cox (4th ed.; New York: Springer-Verlag), 143
Turnshek, D. A., Bohlin, R. C., Williamson, R. L., Lupie, O. L., Koornneef, J., & Morgan, D. H. 1990, AJ, 99, 1243
Vargas Álvarez, C. A., Kobulnicky, H. A., Bradley, D. R., Kannappan, Sh. J., Norris, M. A., Cool, R. J., & Miller, B. P. 2013, AJ, 145, 125
Whittet, D. C. B., Martin, P. G., Hough, J. H., Rouse, M. F., Bailey, J. A., & Axon, D. J. 1992, ApJ, 386, 562
Whittet, D. C. B., & van Breda, I. G. 1978, A&A, 66, 57

R. E. Martínez, A. M. Orsatti, and E. I. Vega: Facultad de Ciencias Astronómicas y Geofísicas, Universidad Nacional de La Plata, C.P. 1900, La Plata, Argentina (ruben, aorsatti, irene@fcaglp.unlp.edu.ar).